CLAS-NOTE 2002-002

METHODS FOR CLOSE-TRACK EFFICIENCY STUDY AND ITS APPLICATION FOR CLAS.

K. Mikhailov*, A. Stavinskiy*, A. Vlassov*

Thomas Jefferson National Accelerator Facility,
12000 Jefferson Avenue, Newport News, Virginia 23606, USA

February 6, 2002

Abstract

We report the results of close track efficiency study for the CLAS detector at Jefferson Laboratory. Three different methods to study efficiency have been used: standard Monte-Carlo simulation within GEANT system, study of correlation function for particles with different masses as a function of relative momenta in laboratory reference system, and event merging. Two of the methods were proposed and used for the first time. The analysis was based on the data sample of the reaction $eA(He^3, He^4, C, Fe) \rightarrow e'h_1h_2X$ obtained by the CLAS detector at initial energy 4.46 GeV(E2 run). It was found that the efficiency decreases strongly when momentum difference is less than 100 MeV/c; the width of the inefficiency region depends on particle momenta at fixed magnetic field value.

*Permanent address: ITEP, B. Cheremushkinskaya 25, 117259 Moscow, Russia

1 Introduction

Some important physics tasks needs particle identification and precise momentum measurements for an extremely hard configuration: two particles with close momenta and the same charge. It is well known that correlations of particles with nearby velocities are sensitive to the space-time distances between the emission points, due to the interference effects and the strong and Coulomb final state interaction[1]. Two-track resolution will limit two particle correlation measurements at small relative momenta, because both particles will hit the same or neighboring detector sells. As a rule, the probability to loss at least one of two tracks is higher, if those tracks are close to each other. Track splitting on the event reconstruction stage is also important but could be rejected using the track quality cut. We will discuss such additional loss of pairs at close momenta in terms of close track efficiency.

We studied close track efficiency for CLAS detector in JLAB. Apart from the traditional Monte-Carlo simulations within GEANT framework, we used two completely new methods to study the efficiency.

One of them is based on the hypothesis that narrow physical singularities are found in the region of close particle momenta in the pair reference system, while technical singularities are expected to be in the region of close particle momenta in the laboratory reference system. For particles with different masses these two regions are different. It means, that one can consider a sharp decreasing of correlation function for particles with different masses at small relative momenta in laboratory reference system as close track efficiency effect[2].

The second method uses artificial events constructed from two real events with well identified protons which momenta are close to each other. Event merging was made on the level of hits(raw data information). These artificial events with close tracks were reconstructed as well as real; the probability of reconstruction provides close track efficiency.

The paper is organized as follows. In Sect.2 short description of CLAS and data sample is presented. Three different methods for study of close track efficiency are described in Sect.3-5 respectively. Comparison between methods are given in the Sect.6. Finally, the conclusions about present status of close track efficiency for CLAS are drawn in Sect.7.

2 Experimental setup and definitions.

Our studies of close track efficiency are concerned with the CLAS detector [3, 4] at the Thomas Jefferson National Accelerator Facility, and partly based on experimental data accumulated by CLAS during E2 run period.

The CLAS detector[4] in Hall B is a six sector toroidal magnetic spectrometer. The magnetic field is generated by six iron-free superconducting coils. The detection systems consist of three drift chamber (DC) regions per sector to determine the trajectories of charged particles [5, 6], scintillator counters (EC) for the trigger and time-of-flight measurements [7], Cherencov counters to distinguish between electrons and negative pions [8], and an electromagnetic shower calorimeter (EC) to identify electrons and neutrons [9, 10].

To study close track efficiency we have used data from E2 run at the energy 4.46 GeV ($e + A \rightarrow e' h_1 h_2 + X$, where A were ^3He,^4He,^{12}C,^{56}Fe, and h_j are π, p, d). The electron

beam current was typically about 10 nA, which yielded a nominal luminosity of about $10^{34} cm^{-2} s^{-2}$, magnetic field was 50 % of maximum value (Torus current 2250 Amps and Minitourus current 6000 Amps).

We define close track efficiency $\varepsilon(q)$ as follows

$$\frac{d\sigma_{measured}}{d\nu dQ^2 d\vec{p_1} d\vec{p_2}} = \varepsilon(q) \cdot \varepsilon_1(\vec{p_1}) \cdot \varepsilon_1(\vec{p_2}) \cdot \frac{d\sigma}{d\nu dQ^2 d\vec{p_1} d\vec{p_2}}, \tag{1}$$

where ν is the energy transfer, Q^2 is the momentum transfer, $\vec{p_1}, \vec{p_2}$ are momenta of particles h_1 and h_2 in the laboratory system, $\vec{q} = \vec{p_1} - \vec{p_2}$ and ε_1 is the single particle reconstruction efficiency. We can extract $\varepsilon(q)$ by studying the ratio:

$$\frac{R_{measured}(q)}{R(q)} = \varepsilon(q) \tag{2}$$

in the processes where no real correlation at small q is expected. Here R is the correlation function which we study for two hadrons with momenta $\vec{p_1}, \vec{p_2}$ in the $(eA, e'h_1h_2X)$ reaction:

$$R(\vec{q}) = \frac{d\sigma/d\nu dQ^2 \cdot d\sigma/d\nu dQ^2 d\vec{p_1} d\vec{p_2}}{d\sigma/d\nu dQ^2 d\vec{p_1} \cdot d\sigma/d\nu dQ^2 d\vec{p_2}} \tag{3}$$

In practice, instead of (3), authors usually use "mixing" [11, 12] procedure to calculate the correlation function:

$$R(\vec{q}) = \frac{N_r(\vec{q})}{N_b(\vec{q})}, \tag{4}$$

where N_r and N_b are the numbers of proton pairs combined from protons taken from the same and different events("mixing" procedure), respectively. The pairs of protons from different events are selected by the same criteria as those from the same event. Both real and mixing distributions are normalized to the same numbers of pairs in the region outside the correlation effect.

For a fixed magnetic field, the track proximity depends not only on q, but also on $p_{12} = |\vec{p_1} + \vec{p_2}|/2$. For this reason we expect certain p_{12} dependence of $\varepsilon(q)$. The example of incorrectly reconstructed close tracks are shown on both parts of Figure 1. The left part of this figure presents detector response for two close momenta protons. Four tracks were reconstructed. This is an example of track splitting. χ^2 criterion of track reconstruction quality provides us the possibility to decide which of them are real tracks and which are artificial ones. The right part of this figure illustrates inefficiency of close tracks reconstruction. One of tracks is not reconstructed correctly and can't pass χ^2 criterion.

First estimation of the close track efficiency was done by visual analysis [13]. The estimation taught us that efficiency is strongly decreased in the region of our interest $q < 100 MeV/c$. We studied the close track efficiency by several methods to get accurate and reliable information on it.

3 Monte-Carlo simulations for study of close track efficiency

In order to estimate the close track efficiency in CLAS detector we have used Monte-Carlo simulation within standard CLAS GEANT[14] simulation package (GSIM)[15]. Two types

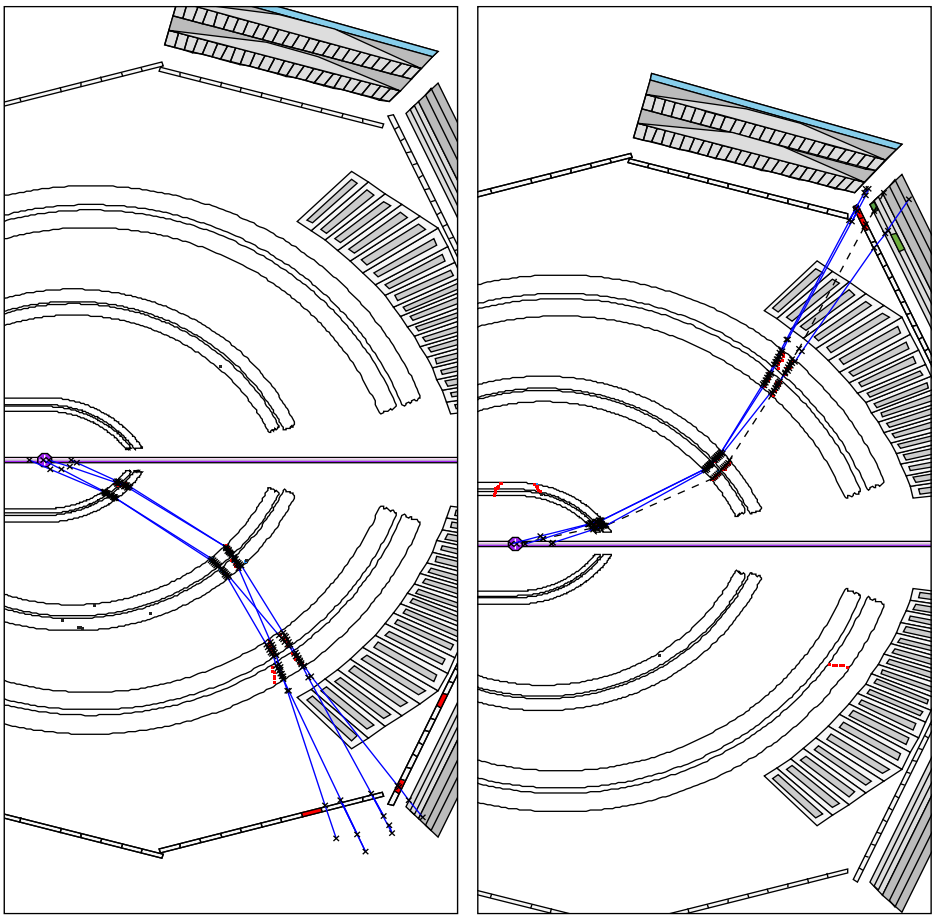

Figure 1: The example of two proton close tracks.

of secondary particle generator was used. For the first type we have simulated reaction $e + 2p \rightarrow e' + 2p + 2\pi$ using phase space generator GENBOD code [16]. Two protons and two pions were generated in the final state to estimate close track efficiency reconstruction for different species of particles in pairs, pp, πp and $\pi\pi$. The kinematical characteristics of this reaction were chosen close to experiment ($Q^2 \sim 1GeV^2$, $\nu \sim 2GeV$). To reproduce experimental spectra of protons in detail we explored second type of generator for GSIM simulation. The two proton events were generated with experimental pair momentum spectrum. This type of generator is more realistic, but on the other hand, the spectra of protons come from reconstructed events, which are already cut by inefficiency. For both types of generator the magnetic field was the same as in experiment (50 % of maximum field value).

The standard version of the CLAS reconstruction and analysis package (RECSIS)[17] was used to reconstruct simulated events. The efficiency was calculated using Equation (2). $R(q)$ was the correlation function of generated events and $R_{measured}(q)$ was the correlation function of reconstructed events. The generated correlation function had no singularities at small q, but it had a slow q-dependence due to kinematical correlations between the generated secondary particles. The event was reconstructed if both scattered electron track and one of the other particles (proton or pion) track passed χ^2 criterion. We took to the analysis the events with proton momentum range 0.3-1.0 GeV/c and with pion momentum range 0.15-0.6 GeV/c. Events with tracks matched the same TOF scintillator were not included in our analysis. This restriction comes from the analysis of the experimental data. Tracks with the same matched scintillator actually had the same time of flight and so far couldn't be reconstructed correctly.

For the proton pairs with $q < 0.1GeV/c$, we divided the pair momentum range by four regions to study the efficiency dependence versus the pair momentum p_{12}. We fitted the efficiency by the function:

$$\varepsilon(q) = a \cdot (1 + bq) \cdot (1 - exp(-\frac{q^2}{\varepsilon_0^2})) \tag{5}$$

Here a is normalization constant, b corresponds to smooth efficiency dependence at relatively large momenta and ε_0 is the width of Gaussian corresponding to the inefficiency at small relative momenta. Several factors (violating of energy and momentum conservation in mixed pairs, possible smooth dependence of the detector efficiency on $\vec{q}$, etc.) lead to a slow growth in the correlation functions on $\vec{q}$. This growth can be separated during data analysis both from interferometry and soft final state interaction effects, which manifest themselves as significantly sharper singularities of the correlation function.

Figure 2 shows the efficiency dependence for the four p_{12} ranges. The Gaussian fits are in agreement with the data within errors. The efficiency parameters ε_0 and χ^2 are shown in the Table 1. One can see that the efficiency parameter ε_0 is increasing with p_{12}. The close track efficiency for πp and $\pi\pi$ pairs was explored using the same fit procedure. The results of the analysis are also shown in the Table 1.

The procedure of extracting of the efficiency for the second type of generator was the same as for the first one. Figure 3 shows $\varepsilon(q)$ dependence for both types of generators. Closed triangles and solid curve are the data and fit corresponding to $e + 2p \rightarrow e' + 2p + 2\pi$. Open triangles and dashed curve correspond to real proton-proton spectrum generator. Particle momentum range for both types of generator was chosen to be the same for comparison. The efficiency parameters ε_0 for both types of generators are in a

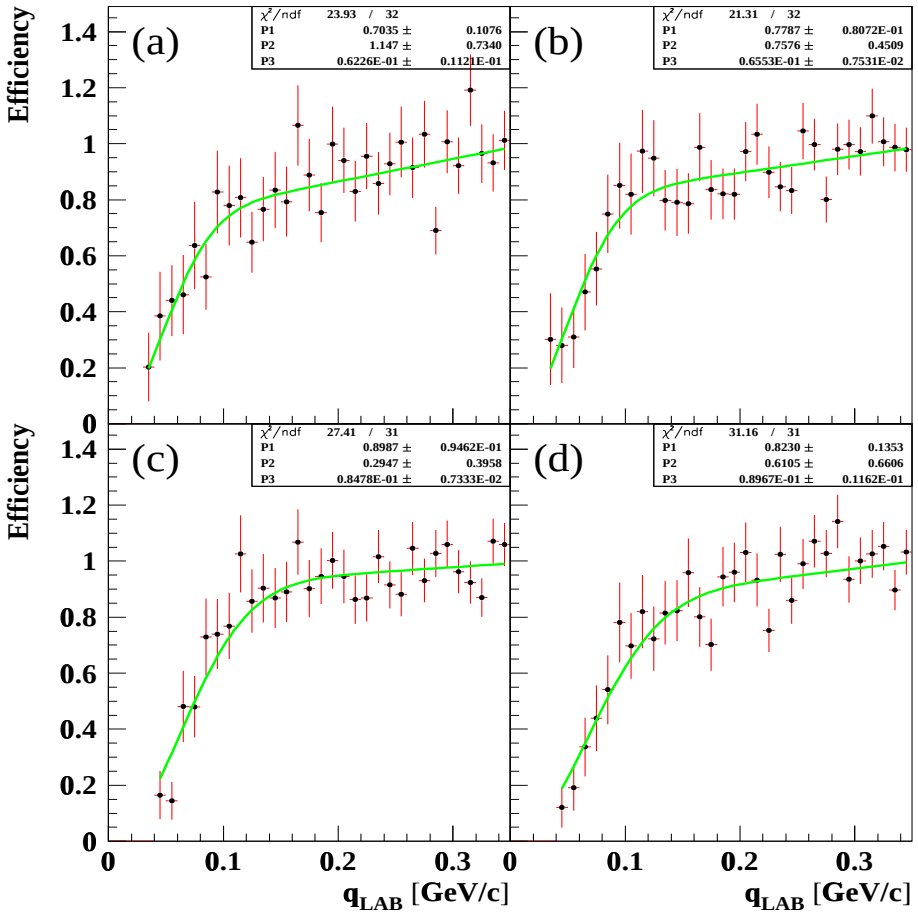

Figure 2: The proton-proton close track efficiency within GSIM for different pair momentum range, generator: $e + 2p \rightarrow e' + 2p + 2\pi$. Mean pair momentum at $q < 0.1$ GeV/c : (a) 0.39 GeV/c, (b) 0.51 GeV/c, (c) 0.63 GeV/c, (d) 0.80 GeV/c

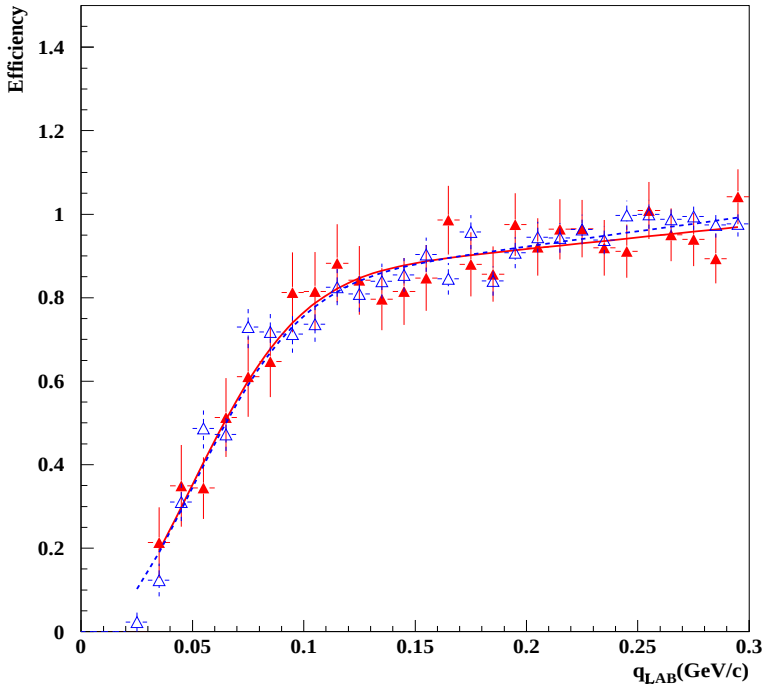

Figure 3: GSIM, generator 1: $e + 2p \rightarrow e' + 2p + 2\pi$ (closed triangles) and fit by equation (5) (solid curve); generator 2: real pp-spectrum (open triangles) and fit by (5) (dashed curve)

good agreement, within statistical and systematic errors. Parameters ε_0 for the second generator for different momentum ranges of protons at $q < 0.1$ GeV/c are shown in Table 2.

4 Study of close track efficiency based on experimental data on $\pi^+ p$ and pd correlations.

The complexity (in comparison with the single-particle detection) in the detection of identical particles with small relative momenta $\vec{q}$ (in the laboratory system) is associated with the fact that the gaps between their tracks are thin not only near the interaction point, but also throughout their lengths. If particles have the same charge and close momenta in the laboratory reference system, but differ significantly in mass, their track proximity will be the same as for identical particles and close track efficiency is expected to be the same. We neglect here a change in momenta through ionization loss and other effects dependent on particle velocities; we also do not consider the case where the trigger gives an advantage to a pair of particles with equal masses.

For a pair of particles with different masses, the soft strong and Coulomb final-state interaction can also be important, but they are concentrated in the other kinematical region characterized by small relative velocities, which means small relative momenta $\vec{k}$ in the rest frame of the pair and invariant masses near the threshold [18]. To our knowledge, there is no reason for sharp singularities to appear in the correlation function of particles with different masses at small relative momenta $\vec{q}$ in the lab.system and no

Table 1: The efficiency parameter ε_0 for pp, πp and $\pi\pi$

$pair$	$< p_{12} >$, GeV/c	$\varepsilon_0 \pm stat.err. \pm syst.err.$	χ^2/ndf
pp	.39	$.062 \pm .011 \pm .005$	24/32
pp	.51	$.066 \pm .008 \pm .003$	21/32
pp	.63	$.085 \pm .007 \pm .002$	27/31
pp	.80	$.090 \pm .011 \pm .006$	31/31
πp	.40	$.078 \pm .007 \pm .007$	37/32
πp	.58	$.095 \pm .011 \pm .009$	31/32
$\pi\pi$	.20	$.061 \pm .007 \pm .008$	39/25
$\pi\pi$	.36	$.070 \pm .007 \pm .005$	21/29

Table 2: E2-spectrum. The efficiency parameter ε_0 for pp

$pair$	$< p_{12} >$, GeV/c	$\varepsilon_0 \pm stat.err. \pm syst.err.$	χ^2/ndf
pp	.35	$.054 \pm .008 \pm .002$	29/31
pp	.41	$.061 \pm .005 \pm .002$	20/26
pp	.50	$.065 \pm .006 \pm .003$	38/26
pp	.68	$.072 \pm .008 \pm .003$	16/26

experimental evidence for their existence is available. We assume that such singularities are negligible, hence physical and methodical singularities for particles with different masses are separated.

The corroboration of such assumption, based on the experimental data will be shown bellow. The detection efficiencies for a pair of identical particles with small relative momenta in the proposed method are determined by measuring the correlation function of particles with different masses and small relative momenta $\vec{q}$. Thus, we suggest that the obtained dependence of such correlation function on the relative momentum $\vec{q}$ can be interpreted as a dependence of the efficiency on $\vec{q}$ [2].

First of all we check our hypothesis that correlation function has no sharp singularities as a function of relative momentum in the C.M. frame k for the region of our study of close track efficiency (small q). Figure 4 shows correlation function for $p\pi^+$ as a function of k for laboratory momentum difference range $0.0 < q < 0.16 GeV/c$. Momentum range for protons was 0.3-1.0 GeV/c, for pions was 0.15-0.6 GeV/c. Correlation function is flat within errors.

Measured dependences of the $p\pi^+$ correlation functions on $\vec{q}$ for $eA \to e' p\pi^+ X$ reaction at 4.46 GeV are shown in Fig.5(a-d).

A decrease of the correlation function at small $\vec{q}$ was interpreted as the efficiency dependence on $\vec{q}$. We shall take it into account by introducing factor $(1 + b\sqrt{q})$, $(1 + bq)$ or $(1 + bq^2)$ in our fit. Finally, fitting the points shown in Fig.5 by a function

$$R = c \cdot (1 + b\sqrt{q}) \cdot (1 - exp(q^2/\varepsilon_0^2)) - fit1 \tag{6}$$

or

$$R = c \cdot (1 + bq) \cdot (1 - exp(q^2/\varepsilon_0^2)) - fit2 \tag{7}$$

or

$$R = c \cdot (1 + bq^2) \cdot (1 - exp(q^2/\varepsilon_0^2)) - fit3 \tag{8}$$

we obtained parameters b, ε_0 and χ^2 values which are presented in Table 3.

The results of the study of parameter dependence on the value of q_{max} are given in the five upper rows of Table 3. As an example of such study the results for carbon are shown. One can see that parameters are stable within errors for fit Eq. 7 while $q_{max} > 0.4 GeV/c$. We fixed $q_{max} = 0.43$ for fit 2 from now on.

The fit results to the $p\pi^+$ for different A and average particle momenta are given in the rows 6-13 of the Table 3. One can see that ε_0 does not depend on mass number of the target A within statistical errors and increases with particle momenta p. The same is valid for pd correlation function(rows 14-17 and Fig.6). For close p (0.48 and 0.44 Gev/c) results for $p\pi^+$ and pd with respect to parameter ε_0 do not differ from each other within errors.

As our interest is focused on the parameter ε_0, we studied the dependence of ε_0 on the way we take into account slow growth of the correlation function at large q. Rows 18-23 show the fit result (Eqs. 6-8) for C and He^4. One can see that ε_0 obtained with different fits spread within the value about 10%. We consider this difference as our systematic uncertainties. As a final value of ε_0 we shall accept the parameters ε_0 from fit by Eq.7. Averaged for different A, our final results for ε_0 are

$p\pi^+, p = 0.34 GeV/c, \varepsilon_0 = 0.052 \pm 0.003 \pm 0.005 GeV/c$

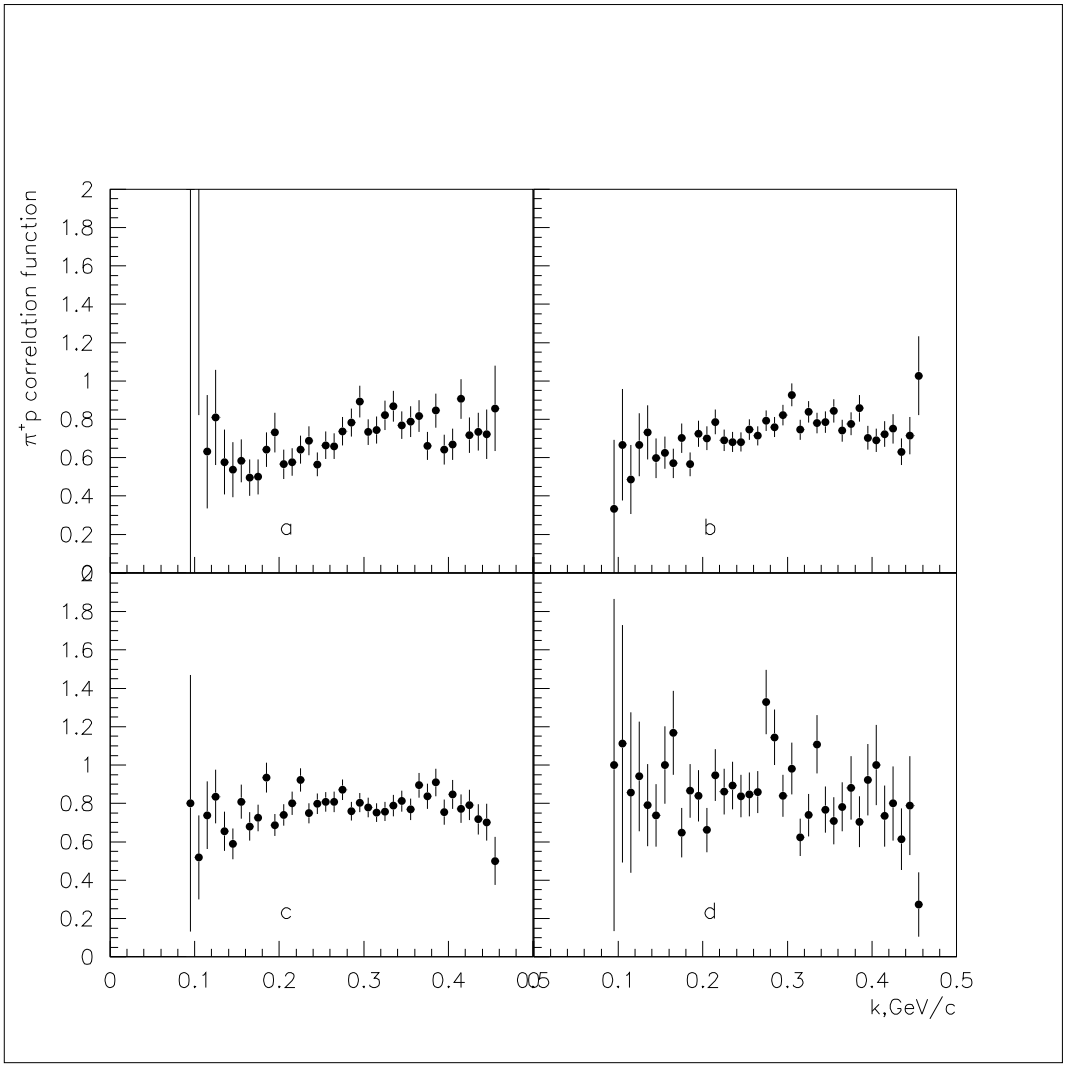

Figure 4: Correlation function for pπ^+ as a function of relative momenta k for laboratory momentum difference range $0.0 < q < 0.16 GeV/c$. a,b,c,d for He^3, He^4, C, Fe targets respectively.

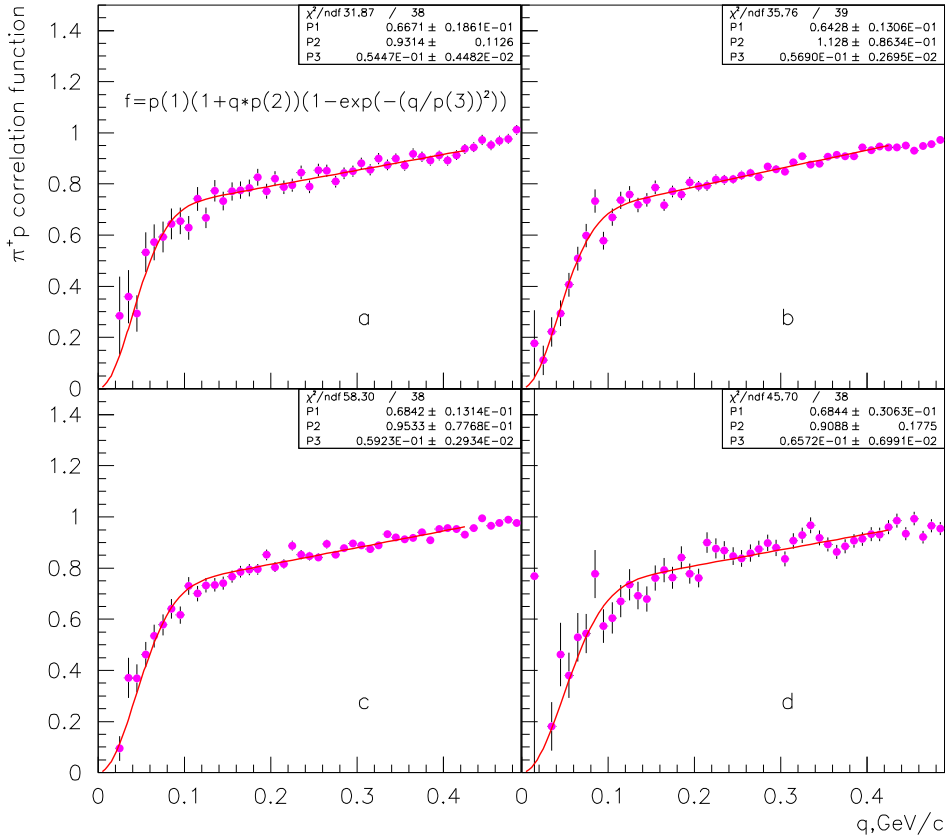

Figure 5: Correlation function for pπ^+ as a function of relative momenta q. a,b,c,d for ^3He, ^4He, ^{12}C, ^{56}Fe targets respectively. Curve represents the best fit result using parameterization (1) with momentum difference range $q < 0.43 GeV/c$. Parameters ε_0 and χ^2 values for different fits are shown in table 3.

Table 3: Results of fits for $p\pi^+$ and pd correlation functions dependencies on q. Average particle momentum p at small q, q_{max} and, as a result, ε_0 in GeV/c

	p	species	A	fit	q_{max}	ε_0	χ^2/ndf
1	.42	$p\pi^+$	C	7	.31	$.054 \pm .003$	32.6/26
2	.42	$p\pi^+$	C	7	.35	$.056 \pm .003$	41.0/30
3	.42	$p\pi^+$	C	7	.39	$.058 \pm .003$	50.4/34
4	.42	$p\pi^+$	C	7	.43	$.059 \pm .003$	58.3/38
5	.42	$p\pi^+$	C	7	.47	$.060 \pm .003$	63.2/42
6	.34	$p\pi^+$	He^3	7	.43	$.042 \pm .007$	33.6/38
7	.34	$p\pi^+$	He^4	7	.43	$.053 \pm .004$	38.8/38
8	.34	$p\pi^+$	C	7	.43	$.052 \pm .004$	27.9/38
9	.34	$p\pi^+$	Fe	7	.43	$.064 \pm .008$	28.2/37
10	.48	$p\pi^+$	He^3	7	.43	$.066 \pm .005$	33.6/38
11	.48	$p\pi^+$	He^4	7	.43	$.065 \pm .004$	42.3/38
12	.48	$p\pi^+$	C	7	.43	$.068 \pm .004$	53.8/38
13	.48	$p\pi^+$	Fe	7	.43	$.071 \pm .011$	40.0/37
14	.44	pd	C	7	.43	$.074 \pm .010$	30.7/38
15	.44	pd	Fe	7	.43	$.068 \pm .011$	26.0/37
16	.60	pd	C	7	.43	$.079 \pm .011$	54.8/37
17	.60	pd	Fe	7	.43	$.078 \pm .014$	28.1/38
18	.60	$p\pi^+$	C	6	.43	$.053 \pm .003$	49.6/38
19	.60	$p\pi^+$	C	7	.43	$.059 \pm .003$	58.3/38
20	.60	$p\pi^+$	C	8	.43	$.067 \pm .003$	79.1/38
21	.60	$p\pi^+$	He^4	6	.43	$.052 \pm .003$	35.5/39
22	.60	$p\pi^+$	He^4	7	.43	$.057 \pm .003$	35.8/39
23	.60	$p\pi^+$	He^4	8	.43	$.063 \pm .003$	46.7/39

$p\pi^+, p = 0.48 GeV/c, \varepsilon_0 = 0.067 \pm 0.002 \pm 0.007 GeV/c$
$pd, p = 0.44 GeV/c, \varepsilon_0 = 0.071 \pm 0.007 \pm 0.007 GeV/c$
$pd, p = 0.60 GeV/c, \varepsilon_0 = 0.079 \pm 0.009 \pm 0.008 GeV/c$

5 Merging

In this method we tried to combine the advantages of the two previous methods: to take events with well-reconstructed protons and well-known proton correlation function (as in GEANT study), and reconstruct them, using real response from CLAS detector elements (as in the case of different mass particle correlation study). As far as the reconstruction procedure for single protons and proton pairs are the same, and single protons were reconstructed, the inefficiency to close tracks can be evaluated.

Such method is sensitive not only to reconstruction procedure but also to the real hardware problems. For example, if there are some ineffective DC wires, the problem will affect both the real, and evaluated efficiency, because we use real raw data information from the detector. The method is good also from the statistical point of view - we can construct enough events for statistical errors to be negligible.

It should be noted that when we merge hits from two events, then DC occupancy is increased, which can result in lower track efficiency. But usually DC occupancy in CLAS is of the order of 1% and it can't affect the efficiency significantly.

The exact procedure was as follows :

- Initial information was the file with reconstructed events, contained both raw data information and reconstructed information such as the type of the secondary particle, it's momentum, track parameters, hit TOF scintillator number, reconstructed start time of the event, etc. Start time is the reconstructed time, so that the difference between measured TOF and start time is real time-of-flight of secondary particle from the target to the detector elements. For runs with initial electron start time is defined by identifying electron and calculating the track length from the target to the detector. We used data from E2 run, in particular, the electron - carbon interactions at 4.46 GeV.

- The track reconstruction procedure is independent for each of 6 sectors of CLAS, so to study proton pair efficiency we selected events with well-reconstructed proton with good track quality (by χ^2 criteria) in a particular sector of CLAS, say sector 1, and electron reconstructed in some other sector. Proton momentum range was $p_{1,2} > 0.3$GeV/c

- Among the selected events the specific pairs of events were selected , where
  - the momentum of reconstructed protons are close.
  - proton tracks from those events don't hit the same TOF scintillator. That restriction came from the real events, where a pair of particles, hitting the same scintillator, was discarded from the analysis, because in such case the measured TOF was wrong for both of them.

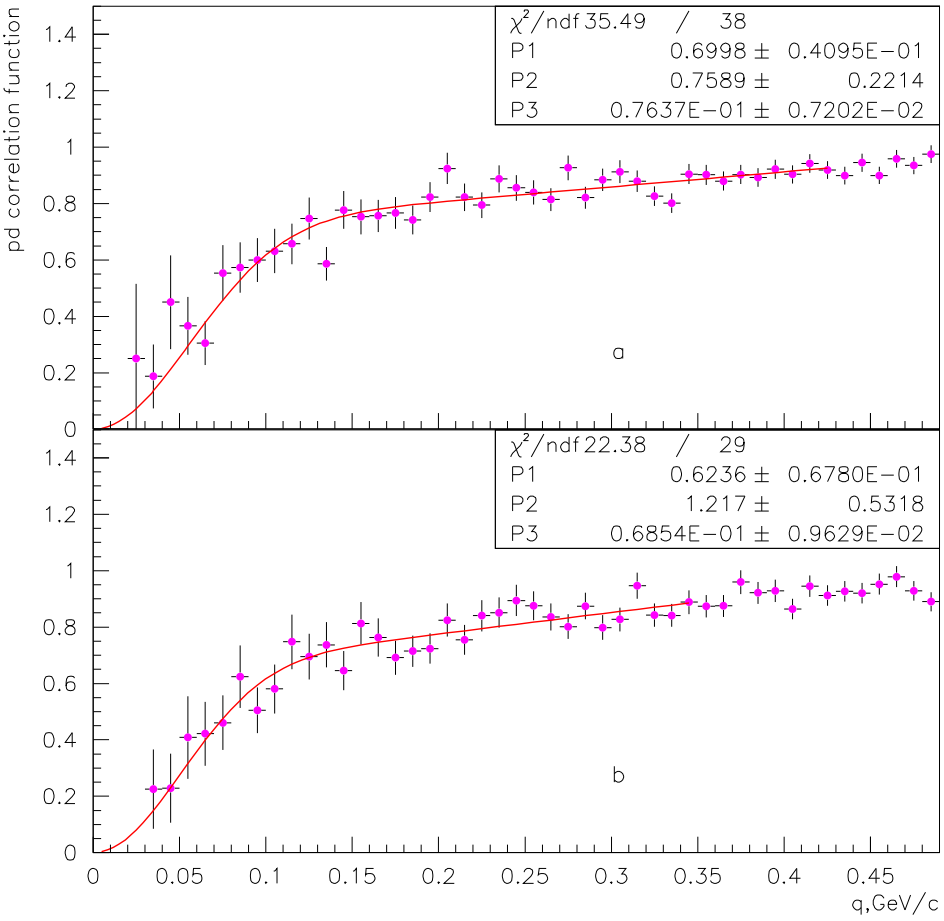

Figure 6: Correlation function for pd as a function of relative momenta q. a,b,c,d for ^3He, ^4He, ^{12}C, ^{56}Fe targets respectively. Curve represents the best fit result using parameterization (1) with momentum difference range $0.02 < q < 0.43 GeV/c$. Parameters and χ^2 values for different fits are shown in Table 3.

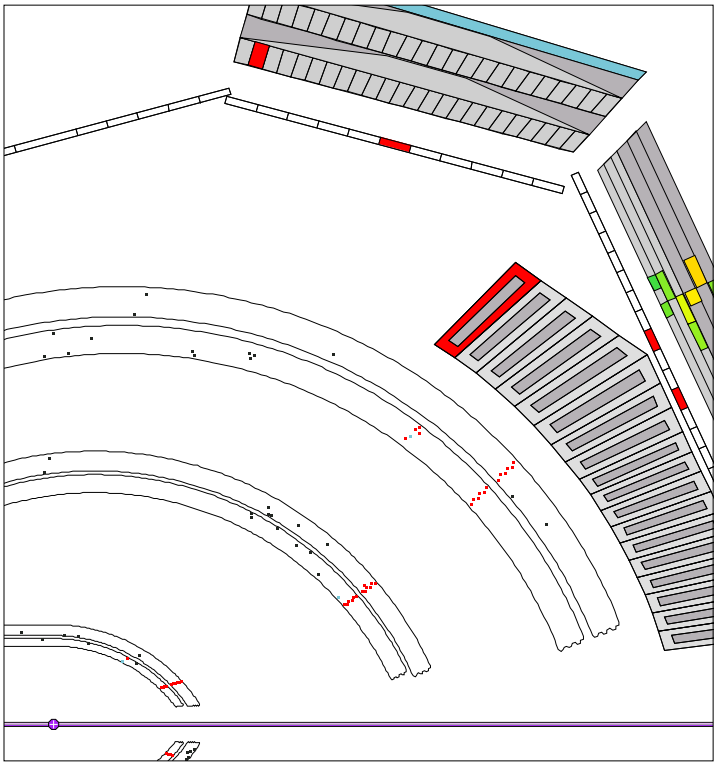

Figure 7: Event **A**

- For those event pairs (Event **A** and **B**) a new event (event **C**) was constructed, where raw data information of sector 1 was the sum of both data from event **A** and **B**. Merging two events into one included the following steps:
  - Event **C** was mostly the same, as event **A**. Only DC and TOF information for sector 1 from event **B** were added to event **A**. Other detectors do not influence the proton reconstruction procedure in this sector.
  - TOF and drift time for event **B** were corrected by the start time difference of the events **B** and **A**.
  - DC information of event **B** can contain the same wire numbers as in event **A**. In such case the drift time was modified to be average of event **B** and **A**. We checked that if we use first time instead, the result will be the same.
- Raw data information of the new event **C** was written to a new file in the same format, as in both events **A** and **B**, so it can be analyzed by the same reconstruction procedure. In addition the information about initially reconstructed proton momenta and some other information needed for later use was stored.

An example of the constructed event can be seen at Figs. 7-9:
Fig. 7 and Fig.8 show sector 1 for events **A** and **B**. One can see proton tracks there. Fig.9 shows merged hits for DC and SC.

As a result, we have the file of events with close proton pairs, which were reconstructed separately by the same reconstruction procedure. The possible reconstruction inefficiency

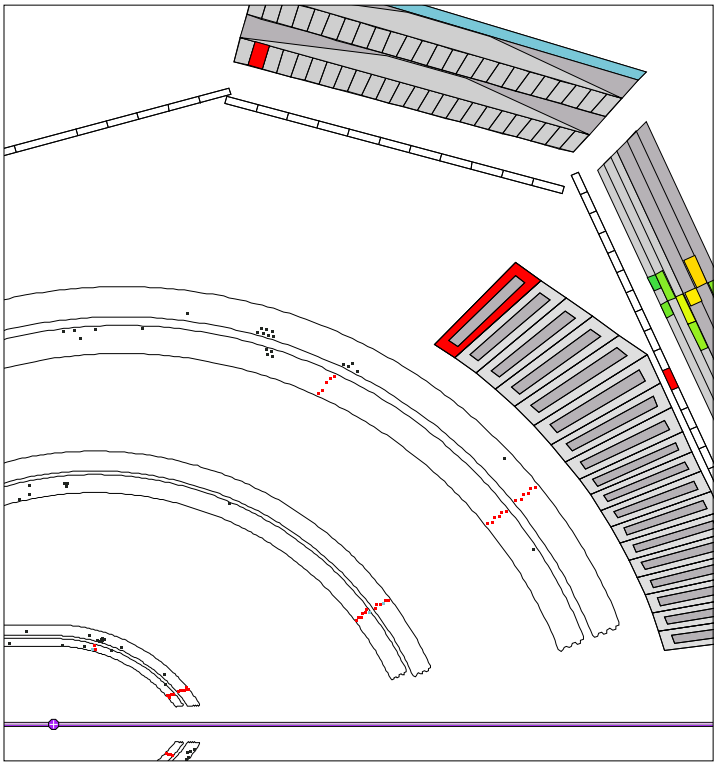

Figure 8: Event **B**

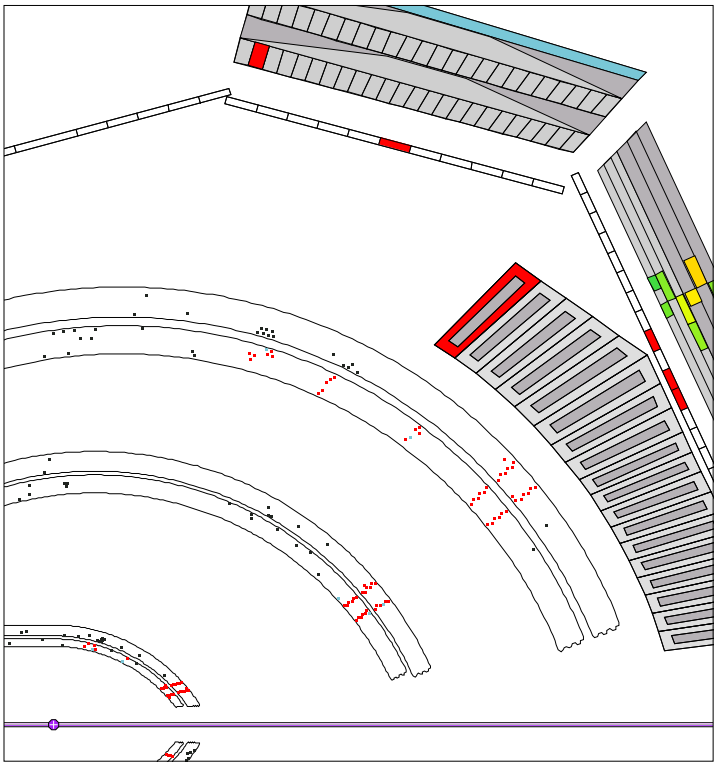

Figure 9: Event **C** as a result of merging events **A** and **B**

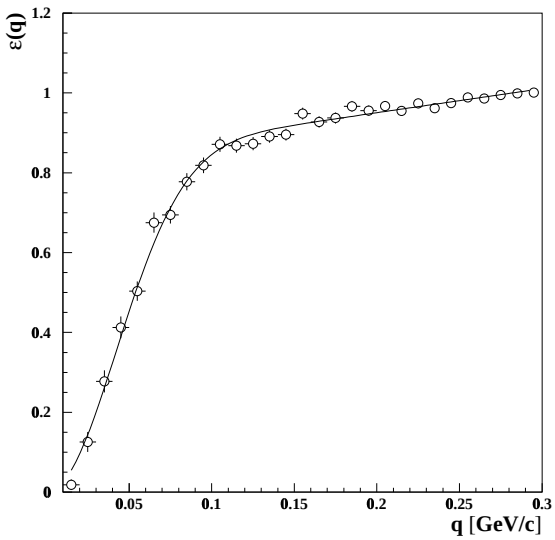

Figure 10: Efficiency for proton pair reconstruction as a function of their momentum difference

Table 4: The efficiency parameter ε_0 for different average proton momenta

pair	$< p_{12} >$, GeV/c	$\varepsilon_0 \pm stat.err. \pm syst.err.$
pp	0.396	$.051 \pm .002 \pm .003$
pp	0.586	$.066 \pm .003 \pm .004$
pp	0.774	$.080 \pm .005 \pm .005$

will be due to small momentum difference of those tracks. Close track efficiency was defined as the ratio of two q distributions : one is a result of pair reconstruction and other was calculated on the basis of single proton reconstruction. This definition is the same as Eq. (1) with $\varepsilon_1 = \varepsilon_2 = 1$.

Fig 10 shows an example of the close track efficiency function.

To study the efficiency dependence on the mean proton momentum p_{12} we divided momentum range on three regions of average proton momentum at $q < 0.1$

The Table 4 shows parameters ε_0 as a function of average proton momenta p_{12} .

6 Discussion.

The dependence of efficiency parameter ε_0 on the average particle momenta p_{12} is shown on figure 11.

One can see from the Figure that parameter ε_0 increases with particle pair momentum. The results obtained by all methods confirm this conclusion. It means that small relative momentum region could be studied using CLAS, but efficiency correction is not negligible and must be obtained with good accuracy.

In order to study detector efficiency with respect to the study of correlation function

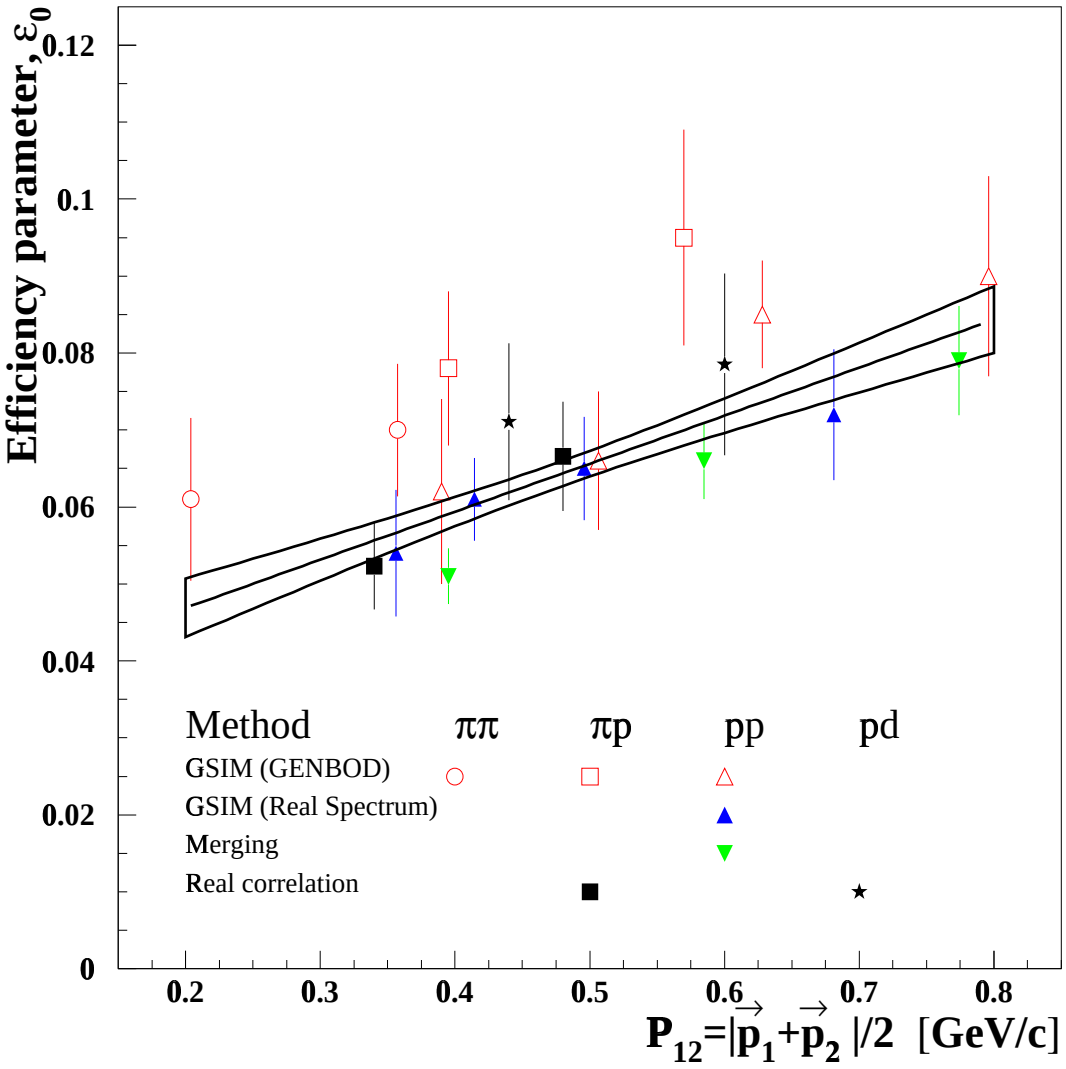

Figure 11: Efficiency parameter for pd,pp,pπ^+, $\pi^+\pi^+$ as a function of mean particle momenta p.

Table 5: Comparison between different methods.

method	a	b	c	statistics
GEANT	excellent	good	very good	very good
real $m_1 \neq m_2$	very good	very good	very good	good
merging	excellent	good	very good	excellent

enhancement at small relative momenta one needs the following conditions:

a) use of well known input correlation function (real or simulated);

b) hardware model should be close to the real detector as possible

c) software should be identical to the real procedure for event reconstruction and calculation of correlation function.

Let's consider to what extent conditions a)-c) are fulfilled for methods we used(see Table 5). And, of course, defining point is statistical accuracy.

Since $p\pi^+$ and pd pairs are not free from other sources of correlations, it could, in principal be the source of systematic uncertainties. For two other methods correlation functions are known.

One can simulate detector properties within GEANT to some extent. Merging do it automatically, but there is a problem to take into account real detector response in the case of overlap hits. Real correlations for particle with different mass are measured by exactly the same detector.

Statistical accuracy for the second method is limited by the real statistics for different mass pairs, which is comparable with statistic for identical pairs. Statistical accuracy for other two methods is in principle unlimited, but merging needs much smaller computer time.

Fortunately, all three methods provide results compatible within statistics and systematics. We consider it as a cross-check of our systematics.

In order to minimize the errors we include the results of all three methods into the fit when studying the particle momentum p_{12} dependence of parameter ε_0. Thus, to our best knowledge, the close track efficiency for CLAS detector in momentum range about $0.3 \div 0.8$ GeV/c is $\varepsilon(p_{12}, q) \sim (1 - exp(\frac{q^2}{\varepsilon_0^2(p_{12})}))$. The average values and errors of parameter ε_0 are shown in Figure 11 (solid and dashed lines) and in Table 6.

Tables number 7,8,9,10 correspond to the efficiency parameter ε_0 calculated for GSIM simulation of reaction $e + 2p \rightarrow e' + 2p + 2\pi$, for GSIM simulation of two protons with experimental momentum spectrum, for experimental data on $\pi^+ p$ and pd correlations and for event merging respectively.

7 Conclusion

1)Detector CLAS and the present variant of reconstruction program provide the possibility to study phenomena at small relative momenta of secondary particles.

2)Simulation of the detector properties within present version of GSIM is reliable with respect to close track reconstruction.

Table 6: The efficiency parameter ε_0 versus p_{12}.

p_{12} GeV/c	ε_0	p_{12} GeV/c	ε_0
0.21	0.475E-01±0.37E-02	0.51	0.662E-01±0.17E-02
0.22	0.482E-01±0.36E-02	0.52	0.669E-01±0.17E-02
0.23	0.488E-01±0.35E-02	0.53	0.675E-01±0.18E-02
0.24	0.494E-01±0.34E-02	0.54	0.681E-01±0.18E-02
0.25	0.500E-01±0.33E-02	0.55	0.687E-01±0.19E-02
0.26	0.506E-01±0.31E-02	0.56	0.694E-01±0.19E-02
0.27	0.513E-01±0.30E-02	0.57	0.700E-01±0.20E-02
0.28	0.519E-01±0.29E-02	0.58	0.706E-01±0.21E-02
0.29	0.525E-01±0.28E-02	0.59	0.712E-01±0.22E-02
0.30	0.531E-01±0.27E-02	0.60	0.719E-01±0.22E-02
0.31	0.538E-01±0.26E-02	0.61	0.725E-01±0.23E-02
0.32	0.544E-01±0.25E-02	0.62	0.731E-01±0.24E-02
0.33	0.550E-01±0.24E-02	0.63	0.737E-01±0.25E-02
0.34	0.556E-01±0.24E-02	0.64	0.744E-01±0.26E-02
0.35	0.563E-01±0.23E-02	0.65	0.750E-01±0.27E-02
0.36	0.569E-01±0.22E-02	0.66	0.756E-01±0.28E-02
0.37	0.575E-01±0.21E-02	0.67	0.762E-01±0.29E-02
0.38	0.581E-01±0.20E-02	0.68	0.768E-01±0.30E-02
0.39	0.588E-01±0.20E-02	0.69	0.775E-01±0.31E-02
0.40	0.594E-01±0.19E-02	0.70	0.781E-01±0.32E-02
0.41	0.600E-01±0.18E-02	0.71	0.787E-01±0.33E-02
0.42	0.606E-01±0.18E-02	0.72	0.793E-01±0.34E-02
0.43	0.613E-01±0.17E-02	0.73	0.800E-01±0.35E-02
0.44	0.619E-01±0.17E-02	0.74	0.806E-01±0.37E-02
0.45	0.625E-01±0.17E-02	0.75	0.812E-01±0.38E-02
0.46	0.631E-01±0.16E-02	0.76	0.818E-01±0.39E-02
0.47	0.637E-01±0.16E-02	0.77	0.825E-01±0.40E-02
0.48	0.644E-01±0.16E-02	0.78	0.831E-01±0.41E-02
0.49	0.650E-01±0.16E-02	0.79	0.837E-01±0.42E-02
0.50	0.656E-01±0.17E-02	0.80	0.843E-01±0.43E-02

Table 7: The efficiency parameter ε_0 versus p_{12} for GSIM simulation of reaction $e + 2p \rightarrow e' + 2p + 2\pi$.

p_{12} GeV/c	ε_0	p_{12} GeV/c	ε_0
0.21	0.608E-01 ±0.69E-02	0.51	0.769E-01 ±0.35E-02
0.22	0.613E-01 ±0.67E-02	0.52	0.775E-01 ±0.36E-02
0.23	0.619E-01 ±0.65E-02	0.53	0.780E-01 ±0.36E-02
0.24	0.624E-01 ±0.63E-02	0.54	0.785E-01 ±0.37E-02
0.25	0.630E-01 ±0.61E-02	0.55	0.791E-01 ±0.38E-02
0.26	0.635E-01 ±0.59E-02	0.56	0.796E-01 ±0.39E-02
0.27	0.640E-01 ±0.58E-02	0.57	0.801E-01 ±0.10E-02
0.28	0.646E-01 ±0.56E-02	0.58	0.807E-01 ±0.41E-02
0.29	0.651E-01 ±0.54E-02	0.59	0.812E-01 ±0.42E-02
0.30	0.656E-01 ±0.52E-02	0.60	0.818E-01 ±0.43E-02
0.31	0.661E-01 ±0.51E-02	0.61	0.823E-01 ±0.45E-02
0.32	0.667E-01 ±0.49E-02	0.62	0.828E-01 ±0.46E-02
0.33	0.672E-01 ±0.48E-02	0.63	0.834E-01 ±0.48E-02
0.34	0.678E-01 ±0.46E-02	0.64	0.839E-01 ±0.49E-02
0.35	0.683E-01 ±0.45E-02	0.65	0.844E-01 ±0.51E-02
0.36	0.689E-01 ±0.44E-02	0.66	0.850E-01 ±0.52E-02
0.37	0.694E-01 ±0.42E-02	0.67	0.855E-01 ±0.54E-02
0.38	0.699E-01 ±0.41E-02	0.68	0.861E-01 ±0.56E-02
0.39	0.705E-01 ±0.40E-02	0.69	0.866E-01 ±0.57E-02
0.40	0.710E-01 ±0.40E-02	0.70	0.871E-01 ±0.59E-02
0.41	0.716E-01 ±0.38E-02	0.71	0.877E-01 ±0.61E-02
0.42	0.721E-01 ±0.37E-02	0.72	0.882E-01 ±0.63E-02
0.43	0.726E-01 ±0.36E-02	0.73	0.887E-01 ±0.64E-02
0.44	0.732E-01 ±0.36E-02	0.74	0.893E-01 ±0.66E-02
0.45	0.737E-01 ±0.35E-02	0.75	0.898E-01 ±0.68E-02
0.46	0.742E-01 ±0.35E-02	0.76	0.906E-01 ±0.70E-02
0.47	0.748E-01 ±0.35E-02	0.77	0.909E-01 ±0.72E-02
0.48	0.753E-01 ±0.35E-02	0.78	0.914E-01 ±0.74E-02
0.49	0.759E-01 ±0.35E-02	0.79	0.920E-01 ±0.76E-02
0.50	0.764E-01 ±0.35E-02	0.80	0.925E-01 ±0.78E-02

Table 8: The efficiency parameter ε_0 versus p_{12} for GSIM simulation of two protons with experimental momentum spectrum.

p_{12} GeV/c	ε_0	p_{12} GeV/c	ε_0
0.35	0.567E-01 ±0.52E-02	0.52	0.652E-01 ±0.38E-02
0.36	0.572E-01 ±0.49E-02	0.53	0.657E-01 ±0.40E-02
0.37	0.577E-01 ±0.47E-02	0.54	0.662E-01 ±0.41E-02
0.38	0.582E-01 ±0.45E-02	0.55	0.667E-01 ±0.43E-02
0.39	0.587E-01 ±0.43E-02	0.56	0.672E-01 ±0.45E-02
0.40	0.592E-01 ±0.41E-02	0.57	0.677E-01 ±0.48E-02
0.41	0.597E-01 ±0.39E-02	0.58	0.682E-01 ±0.50E-02
0.42	0.602E-01 ±0.38E-02	0.59	0.687E-01 ±0.52E-02
0.43	0.607E-01 ±0.37E-02	0.60	0.692E-01 ±0.55E-02
0.44	0.612E-01 ±0.36E-02	0.61	0.697E-01 ±0.58E-02
0.45	0.617E-01 ±0.35E-02	0.62	0.702E-01 ±0.60E-02
0.46	0.622E-01 ±0.34E-02	0.63	0.707E-01 ±0.63E-02
0.47	0.627E-01 ±0.34E-02	0.64	0.712E-01 ±0.66E-02
0.48	0.632E-01 ±0.34E-02	0.65	0.716E-01 ±0.69E-02
0.49	0.637E-01 ±0.35E-02	0.66	0.721E-01 ±0.71E-02
0.50	0.642E-01 ±0.36E-02	0.67	0.726E-01 ±0.74E-02
0.51	0.643E-01 ±0.37E-02	0.68	0.731E-01 ±0.77E-02

Table 9: The efficiency parameter ε_0 versus p_{12} based on experimental data on π^+p and pd correlations.

p_{12} GeV/c	ε_0	p_{12} GeV/c	ε_0
0.33	0.523E-01 ±0.56E-02	0.47	0.668E-01 ±0.44E-02
0.34	0.533E-01 ±0.53E-02	0.48	0.679E-01 ±0.46E-02
0.35	0.543E-01 ±0.50E-02	0.49	0.689E-01 ±0.49E-02
0.36	0.554E-01 ±0.47E-02	0.50	0.700E-01 ±0.52E-02
0.37	0.564E-01 ±0.45E-02	0.51	0.710E-01 ±0.55E-02
0.38	0.575E-01 ±0.42E-02	0.52	0.720E-01 ±0.58E-02
0.39	0.585E-01 ±0.41E-02	0.53	0.731E-01 ±0.61E-02
0.40	0.596E-01 ±0.39E-02	0.54	0.741E-01 ±0.65E-02
0.41	0.606E-01 ±0.39E-02	0.55	0.751E-01 ±0.68E-02
0.42	0.616E-01 ±0.38E-02	0.56	0.762E-01 ±0.72E-02
0.43	0.627E-01 ±0.38E-02	0.57	0.772E-01 ±0.76E-02
0.44	0.637E-01 ±0.39E-02	0.58	0.783E-01 ±0.80E-02
0.45	0.648E-01 ±0.40E-02	0.59	0.793E-01 ±0.84E-02
0.46	0.658E-01 ±0.42E-02	0.60	0.804E-01 ±0.86E-02

Table 10: The efficiency parameter ε_0 versus p_{12} for events merging.

p_{12} GeV/c	ε_0	p_{12} GeV/c	ε_0
0.39	0.508E-01 ±0.35E-02	0.59	0.658E-01 ±0.32E-02
0.40	0.515E-01 ±0.34E-02	0.60	0.665E-01 ±0.33E-02
0.41	0.523E-01 ±0.33E-02	0.61	0.673E-01 ±0.34E-02
0.42	0.530E-01 ±0.32E-02	0.62	0.680E-01 ±0.35E-02
0.43	0.538E-01 ±0.31E-02	0.63	0.688E-01 ±0.36E-02
0.44	0.545E-01 ±0.30E-02	0.64	0.695E-01 ±0.38E-02
0.45	0.553E-01 ±0.29E-02	0.65	0.703E-01 ±0.39E-02
0.46	0.560E-01 ±0.28E-02	0.66	0.710E-01 ±0.41E-02
0.47	0.568E-01 ±0.28E-02	0.67	0.718E-01 ±0.42E-02
0.48	0.575E-01 ±0.27E-02	0.68	0.725E-01 ±0.43E-02
0.49	0.583E-01 ±0.27E-02	0.69	0.732E-01 ±0.45E-02
0.50	0.590E-01 ±0.27E-02	0.70	0.740E-01 ±0.47E-02
0.51	0.598E-01 ±0.27E-02	0.71	0.748E-01 ±0.48E-02
0.52	0.605E-01 ±0.27E-02	0.72	0.755E-01 ±0.50E-02
0.53	0.613E-01 ±0.27E-02	0.73	0.763E-01 ±0.51E-02
0.54	0.620E-01 ±0.28E-02	0.74	0.770E-01 ±0.53E-02
0.55	0.628E-01 ±0.28E-02	0.75	0.778E-01 ±0.55E-02
0.56	0.635E-01 ±0.29E-02	0.76	0.785E-01 ±0.57E-02
0.57	0.643E-01 ±0.30E-02	0.77	0.792E-01 ±0.58E-02
0.58	0.650E-01 ±0.31E-02	0.78	0.800E-01 ±0.60E-02

3)New method for studying close track efficiency, which is based on the study of real correlations for particles with different masses, has been tested successfully; it provides reliable results. An outlook for future applications of the method looks promising. As well as method based on real hard and software without simulations.

4)Another new method for studying close track efficiency, which is based on the event merging procedure, provides results comparable with those from other methods. It looks very promising, because it provides the possibility to study efficiency with practically unlimited statistical accuracy with minimum artificial steps.

5)All three methods, which are used to study close track efficiency, provide the same results with sufficient for practical applications accuracy.

8 Acknowledgments

The authors thank our colleagues from JLAB for their support and hospitality over the years. We particularly wish to thank Nikolai Pivniouk, Pavel Degtiarenko, Volker Burkert, Georgii A. Leksin, Bernhard A. Mecking, Bogdan Niczyporuk, Stepan Stepanyan, Larry Weinstein, Franz Klein, and Mac Mestayer for helpful discussions and remarks. We are also pleased to acknowledge the Department of Energy, USA, for support during our visits to JLAB.

References

[1] G.I.Kopilov and M.I.Podgoretskii,*Sov.J.Nucl.Phys.* **15** (1972) 219;
S.E.Koonin,*Phys.Lett.* **70B** (1977) 43;
R.Lednicky and V.L.Lyuboshits,*Sov.J.Nucl.Phys.* **35** (1982) 770

[2] A.V. Stavinskii,*Inst.and Exp.Tech.* **44-2** (2001) 164

[3] CEBAF Hall B Conceptual Design Report, 1990.

[4] W.Brooks, Nucl.Phys. A 663-664, 1077 (2000); B.Mecking et al., in preparetion.

[5] D.S.Carman et al., NIM A 419, 315 (1998)

[6] M.D.Mestayer et al., NIM A 449, 81 (2000)

[7] E.Smith et al., NIM A 432, 265 (1999)

[8] G.Adams et al., NIM A 465, 414 (2001)

[9] M.Amarian et al., NIM A 460, 239 (2001)

[10] M.Anghinolfi et al., NIM A 447, 424 (2000)

[11] G.I. Kopylov, *preprint JINR P2-7211(1973) in Russian.*

[12] G.I. Kopylov, *Phys. Lett.* **B50** (1974) 472.

[13] CLAS ANALYSIS 1999-004

[14] CERN Program Library Q-123

[15] CLAS NOTE 1993-013

[16] CERN Program Library W-515

[17] CLAS NOTE 1997-003

[18] Boal,D.H. and Shillcock, J.C., *Phys.Rev.* **C33** (1986) 549;
Lednicky,R., Lyuboshits,V.L., Erazmus,B., and Nouais,D., *Phys.Lett.* **B373** (1996) 30